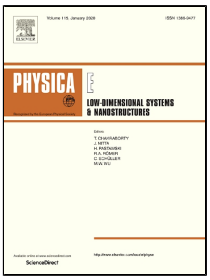

Effect of oxygen atoms on graphene: adsorption and doping

Xinghua Zhu, Kun Liu, Zhibin Lu, Yuanpu Xu, Shunshun Qi, Guangan Zhang

PII:	S1386-9477(19)31378-5
DOI:	https://doi.org/10.1016/j.physe.2019.113827
Reference:	PHYSE 113827
To appear in:	*Physica E: Low-dimensional Systems and Nanostructures*
Received Date:	11 September 2019
Accepted Date:	17 November 2019

Please cite this article as: Xinghua Zhu, Kun Liu, Zhibin Lu, Yuanpu Xu, Shunshun Qi, Guangan Zhang, Effect of oxygen atoms on graphene: adsorption and doping, *Physica E: Low-dimensional Systems and Nanostructures* (2019), https://doi.org/10.1016/j.physe.2019.113827

Effect of oxygen atoms on graphene: adsorption and doping

Xinghua Zhu[a, †], Kun Liu[a, †], Zhibin Lu[a, *], Yuanpu Xu[a], Shunshun Qi[a], Guangan Zhang[a]

[a] State Key Laboratory of Solid Lubrication, Lanzhou Institute of Chemical Physics, Chinese Academy of Sciences, Lanzhou 730000, China

[†] These authors contributed equally to this work.

*Corresponding Author. E-mail: zblu@licp.cas.cn (Z. Lu.)

Abstract

Graphene is an excellent material, which can be used in aerospace field. However, it was reported that when graphene works in an oxygen-rich environment, its surface inevitably absorbs oxygen atoms. And oxygen atoms are doped when graphene has defects. In this study, we investigate the effect of adsorption and doping of oxygen atoms on the properties of graphene using first-principles calculations. We found that the adsorption of single oxygen atom can only change the position of Dirac point. However, the adsorption of multiple oxygen atoms may lead to band gaps. Meanwhile, when graphene has defects, oxygen atoms can repair its lattice. But oxygen atoms also localize some electrons, giving graphene a larger band gap than pure defective graphene. This study is helpful to evaluate the properties of graphene in an oxygen-rich environment. At the same time, it has certain significance for the application of graphene in band gap engineering.

Keywords: Graphene; Oxygen atoms; Band structure; Adsorption; Doping

1. Introduction

Graphene has been a favorite since it was successfully manufactured in the laboratory [1-15]. It is an amazing two-dimensional material that has a lot of great properties, such as strong mechanical strength [16, 17], good thermal conductivity [18], high surface area [3, 19], good electric conductivity [3, 5], etc. These excellent properties enable graphene to show great promise in many applications, such as highly sensitive sensors [11, 12, 20], energy storage and conversion [4, 7, 12], bioscience and biotechnologies [11, 12, 20], smart materials [13], etc.

However, those properties, especially electronic property [21], are affected by the work environment. Because graphene is a form of carbon that has a simple layer of atoms arranged in a honeycomb lattice [18]. This peculiar structure allows graphene to have many interesting properties,

such as quantum spin hall effect [22, 23], coulomb interaction enhancement [24, 25], and weak local inhibition [26], etc.

Thus, many theoretical studies using first-principles methods have begun to elucidate the interaction between doped or non-doped graphene and gases such as water, O_2, N_2, NH_3, CO, NO_2, NO, hydrogen atoms [27-34]. This allows us to understand the microscopic mechanisms that occur at the surface and at the interface. It was reported that for non-doped graphene, different positions of water will cause different atoms in water to react with the surface. This will make the HOMO and LUMO energy levels of water different from the relative position of Dirac point, resulting in different degree of charge transfer and thus different adsorption energy [31]. And it was reported that graphene is highly hydrophobic and the adsorption of water on its surface has little effect on its electronic structure [29]. Charge transfer occurs when graphene adsorbs gas. In this process, water is the acceptor. In other words, charge is transferred to water. But NH_3, CO, NO_2 and NO are the donors, that is, charge is transferred to graphene. Among them, for NH_3, there is little charge transfer, while adsorbed NO_2 will form strong doping, NO will not form strong doping, and only a little charge transfer to NO [31]. For graphene doped with different elements, the type of oxygen adsorption is also different. B- and N-doped are physically adsorbed on graphene, which means that the doped graphene will not be oxidized. While Al-, Si-, P-, Cr-, Mn-doped are chemically adsorbed on graphene. The chemical adsorption of oxygen can change the electronic structure and local spin polarization of doped graphene, in particular, chemical adsorption of O_2 on Cr-doped graphene is antiferromagnetic [27].

However, nowadays studies on graphene surface adsorption mainly focus on a variety of molecules. It was reported that when atomic oxygen was on the surface of graphene, it would adsorb directly above the Bridge point of graphene, with a binding energy of about 2.43 eV [35]. In other words, the graphene surface will inevitably absorb oxygen atoms when it works in an environment containing atomic oxygen. And there is atomic oxygen in low earth orbit [36]. It means that, graphene will inevitably interact with atomic oxygen when it comes to space applications, especially in low earth orbit. And oxygen atoms are much more oxidizing than oxygen molecules, which may adversely affect the aircraft and its internal components. In addition, atomic oxygen at the defect location of graphene will form doping of oxygen atoms when graphene itself has defects. Therefore, it is necessary to study the effect of oxygen atoms on the properties of graphene.

In this study, several comparison groups are established to study the adsorption and doping of oxygen atoms on graphene. Section 3.1 is the study on oxygen atom adsorption, and section 3.2 is about oxygen atom doping. In section 3.1, we studied the effects of different amount of oxygen atom adsorption on the performance of graphene. In addition, when studying the adsorption of multiple oxygen atoms, we also considered the effect of the adsorption position of oxygen atom on graphene performance. In section 3.2, we also considered the effect of the amount of oxygen atoms on the properties of graphene. Meanwhile, we also set up corresponding groups of defective graphene for comparison.

2. Computational methods

This study is based on the density functional plane (DFT) wave pseudopotential method using CASTEP package [37]. A function called Perdew-Burke-Ernzerhof (PBE) of General Gradient Approximation (GGA) is used to describe the exchange-correlation term [38-40]. We use Ultrasoft pseudopotential to replace the real potential of electrons [37]. Method of Grimme is used to correct results in section 3.1 [41, 42]. The cutoff energy for plane wave expansion was set at 500 eV. The SCF convergence threshold was set to 1×10^{-6} eV/atom. In this calculation, 12 Å vacuum space was added to eliminate the periodic effect. In the comparison group, we established a 4×4×1 doped, adsorbed and defect-free supercell. This supercell contains 32 carbon atoms. The other groups were adsorbed, doped or formed defects on the basis of the blank control group. In calculating these supercells, we used a 6×6×1 k-point grid in the Brillouin region. And the shape, size and atomic position of the supercell were optimized so that the force on each ion was less than 0.01 eV/Å and the energy converged to 5×10^{-6} eV/atom.

3. Results and discussion

3.1 Oxygen atom adsorption

3.1.1 One oxygen atom

Figure 1(b) is an optimized model with an oxygen atom adsorbed, and figure 1(d) is the band structure of figure 1(b). The model and band structure of control group are shown in figure 1(a) and (c), respectively. And the population analysis of single oxygen atom adsorption is shown in table 1.

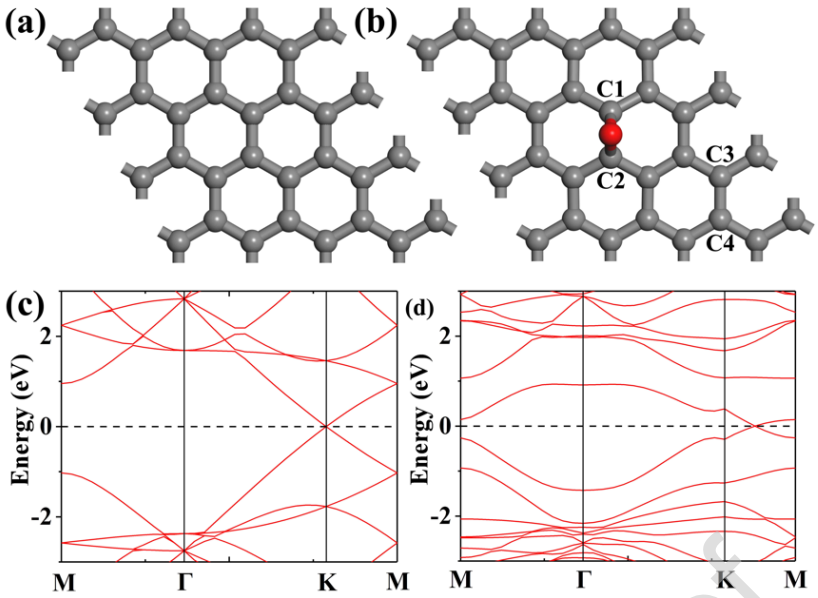

Figure 1. Models and band structures of non-adsorbed and single oxygen atom adsorbed. (a) and (b) are the models of non-adsorbed and single oxygen atom adsorbed respectively, (c) is the band structure of (a), and (d) is the band structure of (b).

Table 1. The bond length and overlapping number in single oxygen atom adsorption model.

Type	C1-C2	C1-O	C3-C4
Bond Length (Å)	1.510	1.466	1.421
Overlap Population	0.53	0.33	1.09

After the optimization, the oxygen atoms are adsorbed directly above bridge site of the graphene, forming a triangle with the two carbon atoms below, as shown in figure 1(b). This phenomenon has been proved by previous study [35]. Two carbon atoms directly below the oxygen atom adsorption site protrude out of the atomic surface of graphene, resulting in a degree of lattice distortion. As can be seen from the figure 1(b), the properties of C1 and C2 carbon atoms in graphene are exactly the same. After oxygen atom adsorption and structure optimization, the bond lengths and overlapping numbers of C1-O and C2-O are still the same, so the two chemical bonds are also exactly the same. Therefore, only one C-O bond is given in the table 1.

The bond strength of C3-C4 slightly away from the adsorption site is relatively high, which is very close to the C-C bond strength in non-adsorbed graphene (bond length: 1.420 Å, overlap population: 1.08), seeing in table 1. For carbon atoms at the adsorption site, the adsorption of oxygen atoms not only weakens the C-C bond directly below, but also slightly lengthens the bond length and decreases the overlap population. Although the overlapping population of the adsorbed oxygen

atom and the carbon atom below is slightly lower, the oxygen atom is still chemically adsorbed from the perspective of bond length and overlapping population. This is because the difference in electronegativity between oxygen and carbon is relatively larger [43, 44]. And oxygen is more oxidising than carbon, which causes the electron cloud to tilt toward oxygen. Oxygen tends to share two electrons with carbon to form a bond because it has six valence electrons, when carbon reacts with oxygen. But in graphene, three of the four valence electrons of a carbon atom are used to form covalent bonds with the surrounding carbon atoms. This allows each carbon atom to provide only one valence electron to form a covalent bond with oxygen. Therefore, the oxygen is going to stick to the bridge point. This allows both carbons to provide a valence electron to form a covalent bond with the oxygen, which stabilizes the structure. In addition, the two carbon atoms involved in the adsorption reaction will be pushed close to the oxygen atoms by the coulomb force, thus protruding the atomic surface of graphene. Oxygen adsorption also reduces the overlap of the electron cloud between C1 and C2, so the bond length of the C1-C2 bond is slightly longer, seeing in table 1.

The band gap of graphene did not change whether atomic oxygen adsorbed or not. But the position of the Dirac cone changed after the oxygen atoms were adsorbed, moving from K to between K and M. The first Brillouin region is a prism with a regular hexagon at the top and bottom, and the section of each regular hexagon in the prism is completely equivalent because a vacuum layer is added vertically in the calculation. That is to say, there will be six Dirac points in the regular hexagon cross section when the oxygen atoms are adsorbed. And after oxygen adsorption, the entire Brillouin band structure will undergo an approximate rotation movement, making the six Dirac points move along the boundary of the regular hexagon for a certain distance. After the move, graphene is still zero-band gap semiconductor.

3.1.2 Two oxygen atoms

The conditions and types of multi-atom oxygen adsorption in graphene are too numerous to be calculated in every case. Therefore, in this study, the adsorption of multi-atom oxygen only considers the adsorption within single six-membered ring. The optimization results show that two oxygen atoms cannot be adsorbed simultaneously above the adjacent C-C bond in single six-element ring. Therefore, for single six-element ring, this study only needs to consider two conditions: meta-dioxide and para-dioxide adsorption. The model and band structure are shown in figure 2.

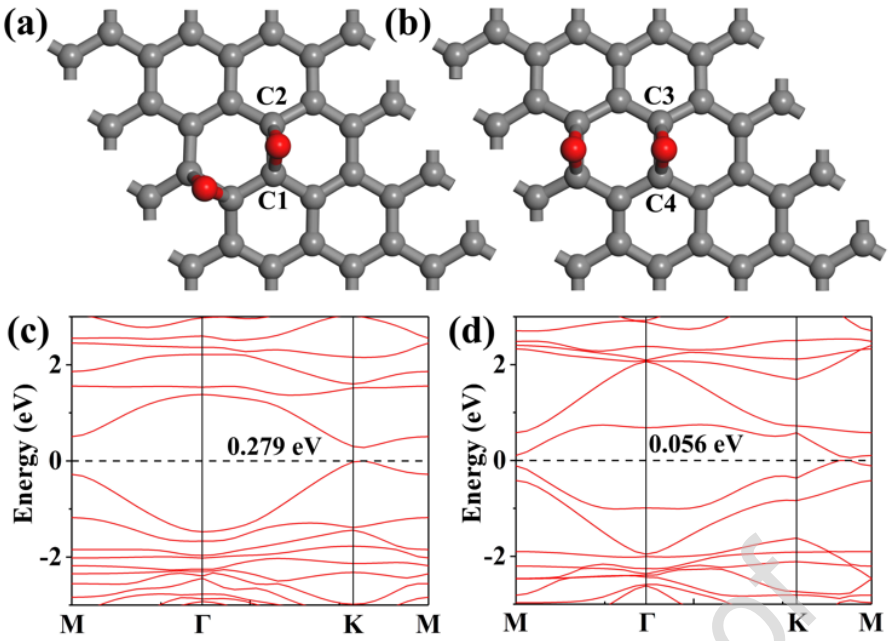

Figure 2. Models and band structures of meta-dioxide and para-dioxide. (a) and (b) are the models of meta-dioxide and para-dioxide respectively, (c) is the band structure of (a), and (d) is the band structure of (b).

In the meta-dioxide adsorption model, two oxygen atoms are completely equivalent, but the two carbon atoms below the same oxygen atom are not equivalent. Therefore, the two covalent bonds of C1 and C2 and oxygen should be discussed separately. The four carbon atoms directly below the two oxygen atoms all protrude from the graphene atomic surface because of coulomb force, indicating that the adsorption of oxygen atoms produces localized lattice distortion. For the chemical bonds at the adsorption position, the bond length and overlapping number after structural optimization are shown in table 2. The results showed that there are slight differences in the bond lengths and the number of overlapping sites between the oxygen and the C1 and C2 bonds, indicating that the strength of the two covalent bonds are different. The C-C bond directly below the oxygen atom is weakened by the oxygen atom's adsorption, and the weakened bond length and bond strength are close to the C-C bond below the oxygen atom when the oxygen atom is adsorbed.

Table 2. The length and overlapping population of the corresponding numbered atoms in the meta-dioxide adsorption model.

Type	C1-O	C2-O	C1-C2
Bond Length (Å)	1.442	1.472	1.505
Overlap Population	0.38	0.32	0.54

In the para-dioxide adsorption model, not only the two oxygen atoms are completely equivalent, but the two carbon atoms directly below the same oxygen atom also have the same properties. Therefore, bond length and overlap number of the two C-O bonds are the same, so they are expressed by C3-O in the table 3.

Table 3. The length of the chemical bond and the number of overlapping populations of the corresponding numbered atoms in the para-dioxide adsorption model.

Type	C3-O	C3-C4
Bond Length (Å)	1.441	1.601
Overlap Population	0.38	0.37

The two bonds of the same oxygen atom are both stronger. However, the C-C bond directly below the adsorbed oxygen atom was seriously damaged, and its bond length became longer. And the number of overlapping populations also decreased significantly. It can be seen from the numerical value of table 3 that the strength of its covalent bond is similar to that of the C-O bond adsorbed on single oxygen atom.

The band structures of meta-dioxide and para-dioxide adsorption are shown in figure 2(c) and 2(d), respectively. It can be seen from figure 1(d) that only one oxygen atom adsorption cannot open the band gap. However, both structures have band gaps. The oxygen atoms make a difference in the properties of the two carbon atoms below the adsorption site, seeing in table 3. This difference makes the carbon atoms below the adsorption site polar. The reason for this phenomenon is that there are covalent bonds between two carbon atoms, which react with different oxygen atoms by adsorption. In other words, C1 is adsorbed to one oxygen atom, and one carbon atom bonded to C1 is adsorbed to another oxygen atom. These two adsorption reactions will interact with each other. However, for C2, it is bonded to one oxygen, but the other carbons that are bonded to C2 are not reacting with the other oxygen. Therefore, this difference in chemical environment leads to the different properties of C1 and C2. This polarity creates an energy gap of 0.279 eV, which eliminates the Dirac cone. And there is also a band gap in the band structure of para-dioxide adsorption, and the band gap value is 0.056 eV. The structure is still a direct band gap structure, but the energy gap is not at three high symmetry points. This band structure is similar to figure 1(d). Then we need to verify whether band gap exists in the M-Γ-K-M path, because the band gap value is very small and

not on the high symmetry point. The total state density of para-dioxide adsorption is shown in figure 3.

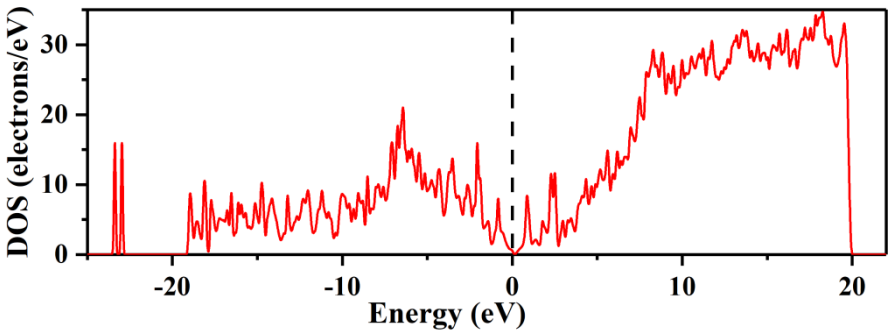

Figure 3. The total density of states of para-dioxide.

In figure 3, there is a state density of 0 at the Fermi level, which indicates that there is a band gap at the Fermi level. In other words, the band gap shown in figure 2(d) is the entire band gap in the first Brillouin region. The band gap is caused by the destruction of the C-C bond directly below the oxygen atom when it is absorbed by para-dioxide, thus slightly damaging the integrity of graphene. When the integrity and continuity of the graphene is broken, the band gap is slightly opened and the Dirac cone disappears.

3.1.3 Three oxygen atoms

The model and band structure of meta-trioxide are shown in figure 4. And table 4 shows the corresponding bond length and overlap population.

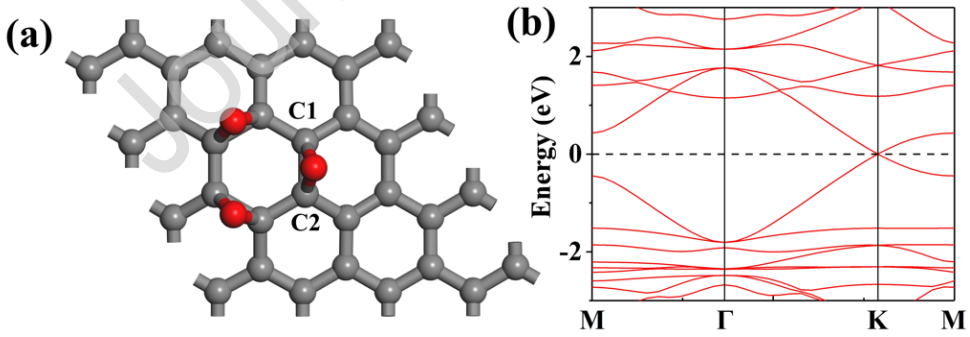

Figure 4. Model and band structure of meta-trioxide. (a) is the model of meta-trioxide, and (b) is the band structure of (a).

Table 4. The bond length and the number of overlap population in the meta-trioxide adsorption model.

Type	C1-O	C1-C2
Bond Length (Å)	1.446	1.510
Overlap Population	0.36	0.52

The structural optimization results showed that the three oxygen atoms are completely equivalent to each other, and so are the two carbons below each oxygen. In other words, three oxygen atoms and six carbon atoms below them form three congruent triangles. The whole adsorption region of oxygen atoms protrudes out of the graphene atomic surface, which means that the adsorption of oxygen introduces some lattice distortion. Since the six C-O bonds and the three C-C bonds below have exactly the same properties, only one C-O bond and one C-C bond are selected to represent all the bonds at the adsorption site, seeing in table 4.

From figure 4 and table 4, C-O bonds and C-C bonds are similar to study 3.1.1. In other words, such adsorption is equivalent to the adsorption of three independent oxygen atoms on graphene. This is because each carbon atom bonds not only with one oxygen atom, but also with a carbon atom that bonds with other oxygen atoms. Each carbon and oxygen atom involved in the adsorption is in the same chemical environment. In this adsorption mode, the graphene is not polarized and its integrity and continuity are not destroyed.

The band structure results showed that the band gap of graphene was not opened and the Dirac cone remained after the adsorption, seeing in figure 4. This result confirmed the previous conclusion that the band gap could not be opened by the adsorption of one oxygen atom. The reason for the opening of the band gap is the polarity generated within graphene, and the integrity and continuity of graphene were destroyed.

3.2 Oxygen doping

3.2.1 One oxygen atom

There are two kinds of oxygen-doped structures. One is the model with single atom vacancy, and the other has a single atomic oxygen doping. The models are shown in figure 5.

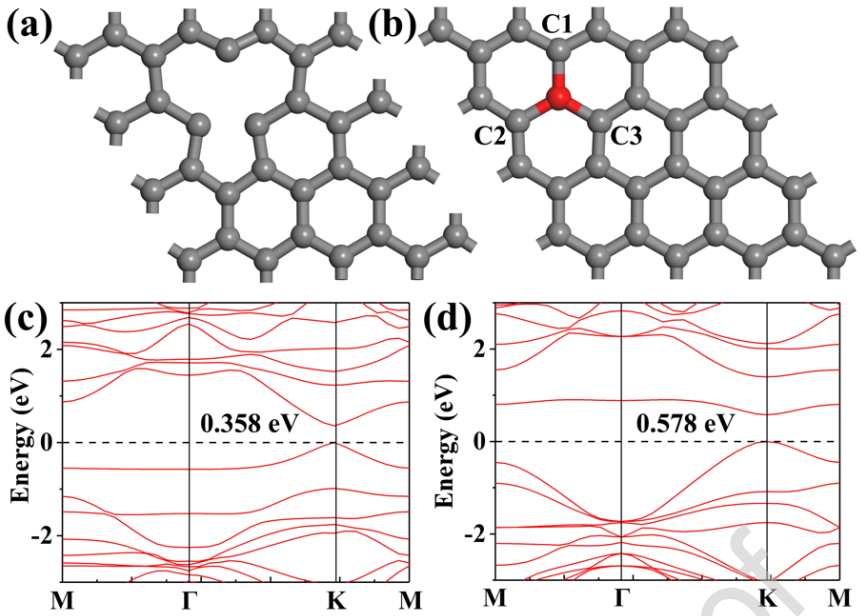

Figure 5. Models and band structures of single atom vacancy and one oxygen atom doped. (a) and (b) are the models of single atom vacancy and one oxygen atom doped respectively, (c) is the band structure of (a), and (d) is the band structure of (b).

Structural optimization results showed that the graphene at the vacancy had some lattice distortion when single atom vacancy existed in graphene. The carbon atoms in the vacancy are close to each other, causing several six-membered rings around the vacancy to deform slightly. However, after absorbing oxygen atoms at the vacancy, the lattice distortion at the defect basically disappears, which indicates that oxygen atoms can repair the lattice structure at the defect. The bond lengths of C1-O, C2-O and C3-O are all the same, with bond lengths of 1.486 eV. And the overlapping population of the three bonds are all equal to 0.49, which means that the chemical bonds of C1-O, C2-O and C3-O are exactly the same.

The integrity and continuity of graphene were destroyed by the vacancy of single atom, so the Dirac cone at point K disappeared and a band gap of 0.358 eV appeared, as shown in figure 5(c). Compared with single-atom defective graphene, the energy level at the bottom of the conduction band tends to be flat after atomic oxygen doping, which means that the doping of atomic oxygen makes the gap in graphene corresponding to this energy band increase locally. And the carrier becomes difficult to transition, thus increasing the energy gap to 0.578 eV.

3.2.2 Multiple oxygen atoms

In this study, the doping of two kinds of multiple oxygen atoms was considered. One is dioxide-doped based on diatomic vacancy, and the other is trioxide-doped with tetratomic vacancy.

Meanwhile, we set up the same atomic defects without doping model as the comparison group. The models and band structures of dioxide-doped are shown in figure 6.

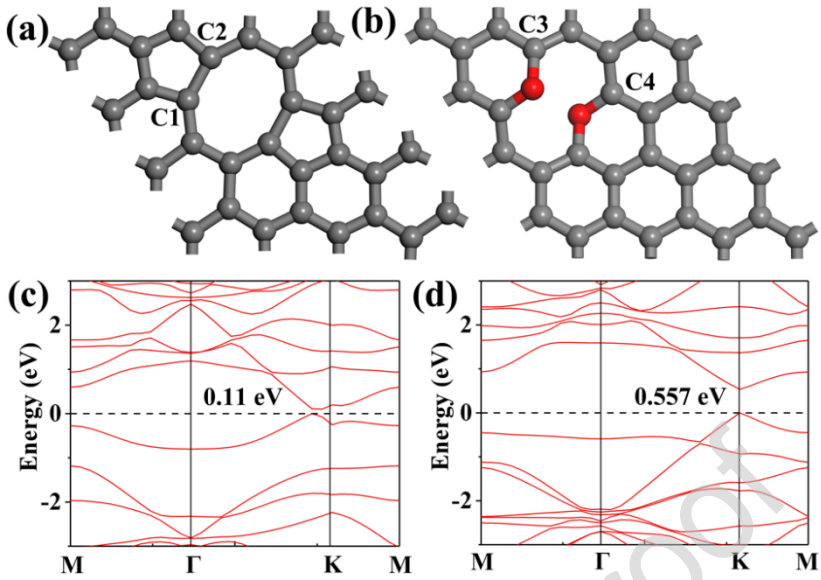

Figure 6. Models and band structures of diatomic defects and dioxide-doped. (a) and (b) are the models with diatomic defects and the dioxide-doped, respectively. (c) and (d) are the band structures of two models.

The two carbons are deleted to form four dangling bonds in diatomic defects model. And the four dangling bonds combine to form two five-membered rings from two six-membered rings that have lost their carbon atoms, seeing in figure 6(a). Two five-membered rings have exactly the same bond length and bond strength. And the bond length of C1-C2 is 1.616 Å, and the overlap population is 0.89. In other word, the new bonds are longer than the C-C bonds found in normal graphene (bond length: 1.420 Å). But they are about as strong as ordinary C-C bonds (overlap population: 1.08). The reason for this is that the formation of the two five-membered rings causes a large lattice distortion around the graphene eight-membered ring formed in the middle.

Two oxygen atoms and four carbon atoms bonded to them are not in the atomic plane of graphene, as shown in figure 6(b). One of the oxygen atoms is sticking up on the atomic plane, and the other is sticking down on the atomic plane, which means that they repel each other. Each oxygen is bonded to two carbons, and two carbons on the same oxygen have the same length and the same strength. However, there is a slight difference between the two C-O bonds, which is 1.388 Å for C3-O and 1.377 Å for C4-O. And the overlapping population of these two bonds is 0.65 and 0.66 respectively. It can be seen from the bond length and strength that the two oxygen atoms should be equivalent, but there may be a slight difference due to the difference in the distance from the boundary of cell or calculation error. If a larger cell is used, the difference can be reduced or

eliminated. But the difference is not significant, so it has little impact on the calculation. In this study, the supercell is still used to calculate the band structure.

Compared with single atom defect, diatomic defect has a smaller band gap, seeing in figure 6(c). This is because the formation of five-membered rings at the defect site is partly equivalent to the repair of graphene. In addition, an eight-membered ring and two five-membered rings replace the suspended bonds of carbon atoms in the diatomic defect model. And in this band structure, the position of band gap deviates from point K, and the band gap value is low. And there is an empty space below the highest valence band with a width of 0.381 eV. Thus, we calculated the density of states. The state density is used to verify whether the band gap value is taken in the Brillouin region path used for calculating the band. And it is also used to observe whether there is an energy level occupying the blank region in the interior of the Brillouin region triangle. The total state density of diatomic defects is shown in figure 7.

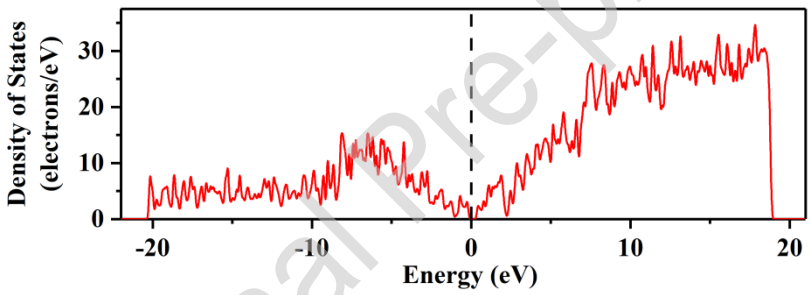

Figure 7. Total state density of diatomic defects

There is a small band gap at the Fermi energy level, so the band gap exists in the Brillouin region path used in this study, seeing in figure 7. In addition, there is a point below the Fermi level that is approximately 0, and this point is a minimum of about 0.5 electron/eV near -1 eV. Therefore, there are occupied states in the blank space below the highest energy level in the valence band, but this occupied state is inside the triangular Brillouin path and is not shown in figure 6(c). The positions of these occupied states in the Brillouin region are not discussed here because they are irrelevant to this study.

As can be seen from the figure 6(d), the doping of oxygen atoms caused the Dirac cone to disappear and opened a band gap of 0.557 eV. However, the position of the band gap has not changed. Moreover, the band curvature at the band gap is still large. In other words, the effective mass of electrons near the Fermi energy level is small. But the appearance of the band gap makes it

more difficult for electrons to transition from valence band to conduction band. The band gap of dioxide-doped is close to and slightly smaller than that of an oxygen atom doping. This indicates that whether the defect is single-oxygen doping or dioxide doping has little difference in the change degree of band gap.

Then, the graphene of trioxide-doped based on the four-atom defect were calculated. The results are shown in figure 8(b) and 8(d). As a control group, the results of four-atom defect are shown in figure 8(a) and 8(c).

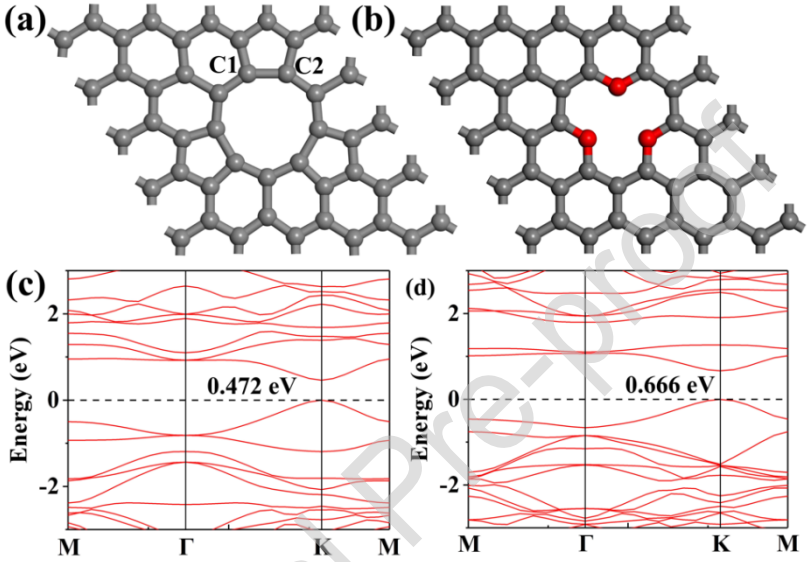

Figure 8. Models and band structures of tetratomic defects and dioxide-doped. (a) and (b) are the models with tetratomic defects and trioxide-doped respectively. (c) and (d) are the band structures of two models respectively

Similar to figure 6, three six-membered rings of lost carbon atoms were reconstituted into five-membered rings after structural optimization. And the newly formed chemical bonds of the other two five-membered rings were identical to C1-C2, seeing in figure 8(a). The covalent bond length of C1 and C2 is 1.619 Å, and the overlap population of the two atoms is 0.95, which means that C1 and C2 atoms form a very stable bond. Therefore, a four-atom defect in graphene ends up being a nine-membered ring at the center, with a five-membered ring around every 120 degrees. And the other six-membered rings all have obvious lattice distortion.

The doping of oxygen does not cause obvious lattice distortion, and all three oxygen atoms are in the graphene atomic plane. And the three oxygen atoms are completely equivalent. The bond length of C-O is 1.373 Å, and the overlap population is 0.68. These values are close to the dioxide-doped, because the dioxide-doped and trioxide-doped is different from the single oxygen atom

doping. For dioxide-doped and trioxide-doped, each oxygen atom only bonds with two carbon atoms, so the overlapping population will be larger and the chemical bond will be more stable.

The band structures of four-atom defect and trioxide-doped are shown in figure 8(c) and 8(d) respectively. The gaps of two models are opened because the continuity of graphene was broken. The band structure of two models is similar, but there are still some differences. In the position of the bottom of conduction band, trioxide-doped is relatively flat, and there are some areas that are not occupied. While the states in the conduction band are continuous in the band structure of four-atom defect. This is because the C1-C2 bond is similar to the ordinary C-C bond, but the C-O bond has a large polarity. Therefore, the localization of the hole at the bottom of the conduction band, effective mass and level flattening of dioxide-doped are increased, compared with the four-atom defect. The curvature of the conductance band bottom and valence band top decreases, and the effective mass of carriers near the Fermi level increases, in the band structure of trioxide-doped, so the energy gap is higher than that of the four-atom defect.

Conclusion

In this study, the first principle is used to study the effect of oxygen atoms on the properties of graphene. Our results reveal that, the adsorption of a single oxygen atom can only change the position of Dirac point in the first Brillouin region. While when multiple oxygen atoms adsorb and interact with each other at the same time, the polarity of graphene will be generated, and even the continuity will be directly destroyed, resulting in small band gaps. On the other hand, the integrity and continuity of graphene can be damaged by defects and oxygen doping, which can open the band gap. Adsorption of 1-3 oxygen atoms at a single site can open a band gap of about 0.6 eV. At the same time, the open band gap value is higher than the pure defect because the doping of oxygen atoms can slightly polarize the graphene. In this study, the effects of atomic oxygen adsorption and doping on the properties of graphene were systematically studied, which is helpful to evaluate the properties of graphene in atomic-oxygen-rich environment. At the same time, it has certain significance for the application of graphene in band gap engineering.

Acknowledgments

The authors are grateful to the National Natural Science Foundation of China (No.51775535 and 11972344) for financial support.

References

[1] K.S. Novoselov, A.K. Geim, S.V. Morozov, D. Jiang, M.I. Katsnelson, I.V. Grigorieva, et al., Two-dimensional gas of massless Dirac fermions in graphene, Nature 438(7065) (2005) 197-200.

[2] A.C. Ferrari, J.C. Meyer, V. Scardaci, C. Casiraghi, M. Lazzeri, F. Mauri, et al., Raman Spectrum of Graphene and Graphene Layers, Physical Review Letters 97(18) (2006) 187401.

[3] F. Schedin, A.K. Geim, S.V. Morozov, E.W. Hill, P. Blake, M.I. Katsnelson, et al., Detection of individual gas molecules adsorbed on graphene, Nature Materials 6 (2007) 652.

[4] M.D. Stoller, S. Park, Y. Zhu, J. An, R.S. Ruoff, Graphene-Based Ultracapacitors, Nano Letters 8(10) (2008) 3498-3502.

[5] A.H. Castro Neto, F. Guinea, N.M.R. Peres, K.S. Novoselov, A.K. Geim, The electronic properties of graphene, Reviews of Modern Physics 81(1) (2009) 109-162.

[6] A.K. Geim, K.S. Novoselov, The rise of graphene, Nanoscience and Technology, Co-Published with Macmillan Publishers Ltd, UK2009, pp. 11-19.

[7] Y. Zhu, S. Murali, M.D. Stoller, K.J. Ganesh, W. Cai, P.J. Ferreira, et al., Carbon-Based Supercapacitors Produced by Activation of Graphene, Science 332(6037) (2011) 1537.

[8] K.S. Novoselov, V.I. Fal′ko, L. Colombo, P.R. Gellert, M.G. Schwab, K. Kim, A roadmap for graphene, Nature 490 (2012) 192.

[9] A.C. Ferrari, D.M. Basko, Raman spectroscopy as a versatile tool for studying the properties of graphene, Nature Nanotechnology 8 (2013) 235.

[10] R.K. Joshi, P. Carbone, F.C. Wang, V.G. Kravets, Y. Su, I.V. Grigorieva, et al., Precise and Ultrafast Molecular Sieving Through Graphene Oxide Membranes, Science 343(6172) (2014) 752.

[11] D. Rodrigo, O. Limaj, D. Janner, D. Etezadi, F.J. García de Abajo, V. Pruneri, et al., Mid-infrared plasmonic biosensing with graphene, Science 349(6244) (2015) 165.

[12] V. Georgakilas, J.N. Tiwari, K.C. Kemp, J.A. Perman, A.B. Bourlinos, K.S. Kim, et al., Noncovalent Functionalization of Graphene and Graphene Oxide for Energy Materials, Biosensing, Catalytic, and Biomedical Applications, Chemical Reviews 116(9) (2016) 5464-5519.

[13] X. Yu, H. Cheng, M. Zhang, Y. Zhao, L. Qu, G. Shi, Graphene-based smart materials, Nature Reviews Materials 2 (2017) 17046.

[14] Y. Cao, V. Fatemi, S. Fang, K. Watanabe, T. Taniguchi, E. Kaxiras, et al., Unconventional

superconductivity in magic-angle graphene superlattices, Nature 556 (2018) 43.

[15] M. Yankowitz, S. Chen, H. Polshyn, Y. Zhang, K. Watanabe, T. Taniguchi, et al., Tuning superconductivity in twisted bilayer graphene, Science 363(6431) (2019) 1059.

[16] C. Lee, X. Wei, J.W. Kysar, J. Hone, Measurement of the Elastic Properties and Intrinsic Strength of Monolayer Graphene, Science 321(5887) (2008) 385.

[17] R.J. Young, I.A. Kinloch, L. Gong, K.S. Novoselov, The mechanics of graphene nanocomposites: A review, Composites Science and Technology 72(12) (2012) 1459-1476.

[18] A.A. Balandin, S. Ghosh, W. Bao, I. Calizo, D. Teweldebrhan, F. Miao, et al., Superior Thermal Conductivity of Single-Layer Graphene, Nano Letters 8(3) (2008) 902-907.

[19] S. Park, R.S. Ruoff, Chemical methods for the production of graphenes, Nature Nanotechnology 4 (2009) 217.

[20] Y. Shao, J. Wang, H. Wu, J. Liu, I.A. Aksay, Y. Lin, Graphene Based Electrochemical Sensors and Biosensors: A Review, Electroanalysis 22(10) (2010) 1027-1036.

[21] B. Huang, Z. Li, Z. Liu, G. Zhou, S. Hao, J. Wu, et al., Adsorption of Gas Molecules on Graphene Nanoribbons and Its Implication for Nanoscale Molecule Sensor, The Journal of Physical Chemistry C 112(35) (2008) 13442-13446.

[22] Y. Zhang, Y.-W. Tan, H.L. Stormer, P. Kim, Experimental observation of the quantum Hall effect and Berry's phase in graphene, Nature 438(7065) (2005) 201-204.

[23] D.A. Abanin, P.A. Lee, L.S. Levitov, Randomness-Induced XY Ordering in a Graphene Quantum Hall Ferromagnet, Physical Review Letters 98(15) (2007) 156801.

[24] D.V. Khveshchenko, Coulomb-interacting Dirac fermions in disordered graphene, Physical Review B 74(16) (2006) 161402.

[25] F. Miao, S. Wijeratne, Y. Zhang, U.C. Coskun, W. Bao, C.N. Lau, Phase-Coherent Transport in Graphene Quantum Billiards, Science 317(5844) (2007) 1530.

[26] S.V. Morozov, K.S. Novoselov, M.I. Katsnelson, F. Schedin, L.A. Ponomarenko, D. Jiang, et al., Strong Suppression of Weak Localization in Graphene, Physical Review Letters 97(1) (2006) 016801.

[27] J. Dai, J. Yuan, Adsorption of molecular oxygen on doped graphene: Atomic, electronic, and magnetic properties, Physical Review B 81(16) (2010) 165414.

[28] T.O. Wehling, A.I. Lichtenstein, M.I. Katsnelson, First-principles studies of water adsorption on graphene: The role of the substrate, Applied Physics Letters 93(20) (2008) 202110.

[29] O. Leenaerts, B. Partoens, F.M. Peeters, Water on graphene: Hydrophobicity and dipole moment using density functional theory, Physical Review B 79(23) (2009) 235440.

[30] S. Casolo, O.M. Løvvik, R. Martinazzo, G.F. Tantardini, Understanding adsorption of hydrogen atoms on graphene, The Journal of Chemical Physics 130(5) (2009) 054704.

[31] O. Leenaerts, B. Partoens, F.M. Peeters, Adsorption of H2O, NH3, CO, NO2, and NO on graphene A first-principles study, Physical Review B 77(12) (2008) 125416.

[32] R. Balog, B. Jørgensen, L. Nilsson, M. Andersen, E. Rienks, M. Bianchi, et al., Bandgap opening in graphene induced by patterned hydrogen adsorption, Nature Materials 9 (2010) 315.

[33] B. Sanyal, O. Eriksson, U. Jansson, H. Grennberg, Molecular adsorption in graphene with divacancy defects, Physical Review B 79(11) (2009) 113409.

[34] Y. Lee, S. Lee, Y. Hwang, Y.-C. Chung, Modulating magnetic characteristics of Pt embedded graphene by gas adsorption (N2, O2, NO2, SO2), Applied Surface Science 289 (2014) 445-449.

[35] M. Topsakal, H. Şahin, S. Ciraci, Graphene coatings: An efficient protection from oxidation, Physical Review B 85(15) (2012) 155445.

[36] M.R. Reddy, Effect of low earth orbit atomic oxygen on spacecraft materials, Journal of Materials Science 30(2) (1995) 281-307.

[37] P. Giannozzi, S. Baroni, N. Bonini, M. Calandra, R. Car, C. Cavazzoni, et al., QUANTUM ESPRESSO: a modular and open-source software project for quantum simulations of materials, Journal of Physics: Condensed Matter 21(39) (2009) 395502.

[38] J.P. Perdew, K. Burke, M. Ernzerhof, Generalized Gradient Approximation Made Simple, Physical Review Letters 77(18) (1996) 3865-3868.

[39] D. Vanderbilt, Soft self-consistent pseudopotentials in a generalized eigenvalue formalism, Physical Review B 41(11) (1990) 7892-7895.

[40] W. Kohn, L.J. Sham, Self-Consistent Equations Including Exchange and Correlation Effects, Physical Review 140(4A) (1965) A1133-A1138.

[41] S. Grimme, Semiempirical GGA-type density functional constructed with a long-range dispersion correction, Journal of Computational Chemistry 27(15) (2006) 1787-1799.

[42] T. Bučko, J. Hafner, S. Lebègue, J.G. Ángyán, Improved Description of the Structure of Molecular and Layered Crystals: Ab Initio DFT Calculations with van der Waals Corrections, The Journal of Physical Chemistry A 114(43) (2010) 11814-11824.

[43] G. Simons, M.E. Zandler, E.R. Talaty, Nonempirical electronegativity scale, Journal of the American Chemical Society 98(24) (1976) 7869-7870.

[44] R.T. Sanderson, Electronegativity and bond energy, Journal of the American Chemical Society 105(8) (1983) 2259-2261.

Author Statement

Xinghua Zhu：Conceptualization; Methodology; Investigation; Writing - Original Draft; Writing-Review & Editing

Kun Liu：Conceptualization; Methodology; Writing-Original Draft;

Zhibin Lu：Conceptualization; Methodology; Writing-Review & Editing; Funding acquisition

Yuanpu Xu：Investigation

Shunshun Qi：Investigation

Guangan Zhang：Funding acquisition

Declaration of interests

☒ The authors declare that they have no known competing financial interests or personal relationships that could have appeared to influence the work reported in this paper.

☐The authors declare the following financial interests/personal relationships which may be considered as potential competing interests:

1. Adsorption of oxygen atoms on graphene with different defect types are calculated.
2. Adsorption of single oxygen atoms can only change the position of the Dirac point.
3. Adsorption of multiple oxygen atoms may lead to band gaps.
4. Oxygen atoms can localize electrons, making graphene's band gap even larger.